

# Induced fermionic current by a magnetic tube in the cosmic spacetime

M. S. Maior de Sousa <sup>\*</sup>, R. F. Ribeiro <sup>†</sup> and E. R. Bezerra de Mello <sup>‡</sup>

Departamento de Física-CCEN  
Universidade Federal da Paraíba  
58.059-970, J. Pessoa, PB  
C. Postal 5.008  
Brazil

June 26, 2021

## Abstract

In this paper, we consider a charged massive fermionic quantum field in the space-time of an idealized cosmic string, in the presence of a magnetic field confined in a cylindrical tube of finite radius. Three distinct configurations for the magnetic field is taken into account: (i) a cylindrical shell of radius  $a$ , (ii) a magnetic field proportional to  $1/r$  and (iii) a constant magnetic field. In these three cases, the axis of the infinitely long tube of radius  $a$  coincides with the cosmic string. Our main objective is to analyze the induced vacuum fermionic current densities outside the tube. In order to do that, we explicitly construct the wave-functions inside and outside the tube for each case. Having the complete set of normalized wave-functions, we use the summation method to develop our analysis. We show that in the region outside the tube, the induced currents are decomposed into a parts corresponding to a zero-thickness magnetic flux in addition to a core-induced contributions. The latter presents specific form depending on the magnetic field configuration considered. We also see that the only non-vanishing component of fermionic current corresponds to the azimuthal one. The zero-thickness contribution depends only on the fractional part of the ration of the magnetic flux inside the tube by the quantum one. As to the core-induced contribution, it depends on the total magnetic flux inside the tube, and consequently, in general, it is not a periodic function of the flux.

PACS numbers: 11.27.+d, 04.62.+v, 98.80.Cq

## 1 Introduction

The existence of a magnetic flux tube penetrating a type II superconductor, named **vortex**, was first demonstrated by Abrikosov [1], by using the Ginzburg-Landau theory of superconductivity. Some years later, Nielsen and Olesen [2] have shown, by using a classical relativistic field theory, composed by Higgs fields interacting with Abelian one, that presents spontaneously gauge symmetry broken, contains static cylindrically symmetric solution carrying a magnetic flux. This configuration corresponds to the vortex solution. The equations of motion associated for this

---

<sup>\*</sup>E-mail: kael Sousa@gmail.com

<sup>†</sup>E-mail: rfreire@fisica.ufpb.br

<sup>‡</sup>E-mail: emello@fisica.ufpb.br

system form a set of coupled non-linear differential equation, that, in general, has no closed solutions. The analysis of the influence of this system on the geometry of the spacetime was analyzed numerically by Garfinkle [3] and Laguna [4] many years ago. In these papers the authors showed that, the vortex has a inner structure characterized by a non-vanishing core carrying a magnetic flux, whose extension is determined by the energy scale where the symmetry is broken. Two length scales naturally appear, the one related with the extension of the magnetic flux proportional to the inverse of vector field mass,  $m_v$ , and the other associated with the inverse of the scalar field mass,  $m_s$ . The latter being the radius that the scalar field reaches its vacuum value. Moreover the authors also verify that asymptotically the surface perpendicular to the vortex corresponds to a Minkowski one minus a wedge. A special vortex solution that satisfy the Bogomolnyi-Prasad-Somerfield (BPS) limit, presents both masses equal, i.e.,  $m_v = m_s$ . For this case Linet [5] was able to find, in the infinity electric charge and Higgs field self-coupling limit, exact solution for the metric tensor, which is determined in terms of the linear energy density of the string. In this limit, the surface perpendicular to the vortex-line solution has a conical structure, and the space around this object corresponds to an idealized cosmic string.

According to the Big Bang theory, the universe has been expanding and cooling. During its expansion, the spontaneous breaking of fundamental symmetries leads the universe to a series of phase transitions. In most interesting model of high-energy physics, the formation of topological defects such as domain walls, monopoles, cosmic string, among others are predicted to occur [6]. These topologically stable structures have a number of interesting observable consequences, the detection of which would provide an important link between cosmology and particle physics. The cosmic strings are among the various type of topological defects, the most studied. Though the recent observations of the cosmic microwave background radiation have ruled out them as the primary source for primordial density perturbations, cosmic strings give rise to a number of interesting physical effects such as gamma rays bursts [7], the emission of gravitational waves [8] and the generation of high-energy cosmic rays [9]. String-like defects also appear in a number of condensed matter systems, including liquid crystals and graphene made structures.

The complete analysis of the behavior of a quantum charged field in the neighborhood of an Abelian Nielsen and Olesen (NO) string must take into account not only the influence of the geometry of the spacetime, but also the influence of the magnetic field. Two distinct analysis can be mentioned: (i) The first one is to consider the string as an idealized linear topological defect, having a magnetic field running along it. This case can be treated analytically. (ii) The second approach is to consider the non-zero thickness for the string. Unfortunately this problem is analytically intractable. In the idealized model, the conical structure of the spacetime modifies the zero-point vacuum fluctuation of quantized fields inducing non-vanishing vacuum expectation values (VEV) for important physical observable. This analysis has been developed in many papers for scalar, fermionic and electromagnetic fields (see, for instance, references given in [10]); moreover considering the presence magnetic flux, additional polarization effects associated with charged quantum fields take place [11]-[14]. In particular this magnetic flux induces non-vanishing current densities,  $\langle j^\mu \rangle$ . This phenomenon has been investigated for scalar fields in Ref.[15, 16]. The analysis of induced fermionic currents in higher-dimensional cosmic string spacetime in the presence of a magnetic flux have been developed in Ref. [17]. In all these analysis, the authors have shown that induced vacuum current densities along the azimuthal direction appear if the ratio of the magnetic flux by the quantum one has a nonzero fractional part. Moreover, induced fermionic and scalar current densities in compactified cosmic string spacetimes have been considered in [18] and [19].

Because the analysis of a quantum system in a realistic model for the NO vortex cannot be exactly analyzed, an intermediate approach is to assume an approximated model for this string, that consists to consider the spacetime produced by the string as being conical everywhere, but having a non-zero thickness magnetic field surrounding it. In this way, some improvements

were obtained in the calculations of the VEV of some physical observable when compared with the idealized case. This approach was used in [20, 21] to calculate the VEV of charged scalar and fermionic energy-momentum tensor, respectively.<sup>1</sup> More recently the scalar vacuum current induced by a magnetic flux in a cosmic string considering a non-vanishing core has been developed in [23]. In these calculations the vacuum polarization effects present two contributions. The first one associated with a zero-thickness magnetic flux. This contribution is a periodic function of the magnetic flux inside the tube, with the period equal to the quantum flux. The second contribution, named core-induced contribution, is not a periodic function of the flux. In fact the core-induced contribution depends on the total magnetic flux inside the core. Three different configurations of magnetic flux that allow us to obtain exact wave-function solutions were considered: (i) A magnetic field on a cylindrical shell, (ii) a magnetic field proportional to  $1/r$ , and finally (iii) a homogeneous magnetic field inside the tube.

Motivated by these results, we decided in this paper to analyze the induced fermionic current density in the system defined above, i.e., an idealized cosmic string surrounded by a magnetic field confined in a tube of finite radius. In order to do that we shall explicitly calculate the wave-functions inside and outside the tube for each case, and by the summation method we shall develop the calculation of induced fermionic current.

This paper is organized as follow. In section 2 we describe the background geometry of the spacetime and the configuration of the magnetic fields. We provide the general structure of the complete set of normalized positive- and negative-energy fermionic mode functions, which can be adapted for each magnetic field configuration. These functions obey the continuity boundary on the surface of the cylindrical tube of radius  $a$ . In section 3, by using the mode-summation method, we show that the VEVs for the charge density, the radial and axial current densities vanish. Only azimuthal current density is induced. Then we evaluate the renormalized VEV of this current density. We show that the later can be decomposed in two parts: The first one corresponds to the induced current by a zero-thickness magnetic flux in the geometry of an idealized cosmic string, and the second one is induced by the non-zero core of the magnetic tube. The latter is calculated, separately, for the three kinds of magnetic flux considered. The behavior of them are discussed in various asymptotic regions of the parameters. We also present some plots associated with the core-induced azimuthal current exhibiting its behavior as function of the most relevant physical variables. Our most relevant conclusions are summarized in section 4. In the appendix A we present some recurrence relations involving Whittaker functions  $M_{\kappa,\mu}(z)$ , needed by us to construct the fermionic wave-functions in a simpler form. We would like to point out that these relations were not found in the literature. Because these relations may be useful for anybody else in the future, we decided to explicitly present them. Throughout the paper we use the units with  $G = \hbar = c = 1$ .

## 2 The geometry and the fermionic wave-functions

The background geometry associated with an idealized cosmic string along the  $z$ -axis, can be given, by using cylindrical coordinates, through the line element below:

$$ds^2 = dt^2 - dr^2 - r^2 d\phi^2 - dz^2, \quad (2.1)$$

where the coordinates take values in range  $r \geq 0$ ,  $0 \leq \phi \leq \phi_0 = 2\pi/q$ ,  $-\infty \leq t \leq +\infty$  and  $-\infty \leq z \leq +\infty$ . The parameter  $q$  associated with the planar angle deficit is related to the mass per unit length of the string,  $\mu_0$ , by  $q^{-1} = 1 - 4\mu_0$ .

---

<sup>1</sup>Allen et al [22] have analyzed the vacuum polarization effect of a massless scalar field on a cosmic string spacetime, considering generically the effect of the strings core through the non-minimal coupling between the scalar field with the geometry.

The quantum dynamic of a massive charged spinor field in curved space-time and in the presence of an electromagnetic four-vector potential,  $A_\mu$ , is described by the Dirac equation,

$$i\gamma^\mu(\nabla_\mu + ieA_\mu)\psi - m\psi = 0, \quad \nabla_\mu = \partial_\mu + \Gamma_\mu, \quad (2.2)$$

where  $\gamma^\mu$  are the Dirac matrices in curved space-time and  $\Gamma_\mu$  is the spin connection. Both matrices are given in terms of the flat space-time Dirac matrices,  $\gamma^{(a)}$ , by the relations

$$\Gamma_\mu = -\frac{1}{4}\gamma^{(a)}\gamma^{(b)}e_{(a)}^\nu e_{(b)\nu;\mu}, \quad \gamma^\mu = e^\mu_{(a)}\gamma^{(a)}. \quad (2.3)$$

In the above expression  $e^\mu_{(a)}$  represents the basis tetrad satisfying the relation  $e^\mu_{(a)}e^\nu_{(b)}\eta^{ab} = g^{\mu\nu}$ , with  $\eta^{ab}$  being the Minkowski space-time metric tensor.

The system that we want to analyse takes into account three different configurations of magnetic fields. They are: (i) A magnetic field on a cylindrical shell of radius  $a$ , (ii) a magnetic field proportional to  $1/r$ , and finally (iii) a homogeneous magnetic field inside the tube. In these three cases, the axis of the infinitely long tube of radius  $a$  coincides with the cosmic string. In order to reproduce these three configurations of magnetic field and proceed with our calculations, we consider the potential vector given by

$$A_\mu = (0, 0, A_\phi(r), 0), \quad (2.4)$$

with

$$A_\phi(r) = -\frac{q\Phi}{2\pi}a(r). \quad (2.5)$$

For the first model,

$$a(r) = \Theta(a - r). \quad (2.6)$$

For the two second models, we can represent the radial function  $a(r)$  by:

$$a(r) = f(r)\Theta(a - r) + \Theta(r - a), \quad (2.7)$$

with

$$f(r) = \begin{cases} r/a, & \text{for the second model,} \\ r^2/a^2, & \text{for the third model.} \end{cases} \quad (2.8)$$

In the expressions above,  $\Theta(z)$  represents the Heaviside function, and  $\Phi$  the total magnetic flux.

To find the complete set of mode of fermionic wave-functions for the problem under consideration, we shall use the standard representation of the flat space Dirac matrices:

$$\gamma^{(0)} = \begin{pmatrix} 1 & 0 \\ 0 & -1 \end{pmatrix}, \quad \gamma^{(a)} = \begin{pmatrix} 0 & \sigma^a \\ -\sigma^a & 0 \end{pmatrix}, \quad a = 1, 2, 3, \quad (2.9)$$

with  $\sigma^1$ ,  $\sigma^2$  and  $\sigma^3$  being the Pauli matrices. We take the tetrad basis as follow:

$$e^\mu_{(a)} = \begin{pmatrix} 1 & 0 & 0 & 0 \\ 0 & \cos(q\phi) & -\sin(q\phi)/r & 0 \\ 0 & \sin(q\phi) & \cos(q\phi)/r & 0 \\ 0 & 0 & 0 & 1 \end{pmatrix}, \quad (2.10)$$

where the index  $(a)$  identifies the rows of the matrix. With this choice, the gamma matrices take the form

$$\gamma^0 = \gamma^{(0)} = \begin{pmatrix} 1 & 0 \\ 0 & -1 \end{pmatrix}, \quad \gamma^l = \begin{pmatrix} 0 & \sigma^l \\ -\sigma^l & 0 \end{pmatrix}, \quad (2.11)$$

where we have introduced the  $2 \times 2$  matrices for  $l = (r, \phi, z)$ :

$$\sigma^r = \begin{pmatrix} 0 & e^{-iq\phi} \\ e^{iq\phi} & 0 \end{pmatrix}, \quad \sigma^\phi = -\frac{i}{r} \begin{pmatrix} 0 & e^{-iq\phi} \\ -e^{iq\phi} & 0 \end{pmatrix}, \quad \sigma^z = \begin{pmatrix} 1 & 0 \\ 0 & -1 \end{pmatrix}. \quad (2.12)$$

For this case the spin connection and combination appearing in the Dirac equation we find

$$\Gamma_\mu = \frac{1-q}{2} \gamma^{(1)} \gamma^{(2)} \delta_\mu^\phi, \quad \gamma^\mu \Gamma_\mu = \frac{1-q}{2r} \gamma^r. \quad (2.13)$$

Then the Dirac equation take the form

$$\left( \gamma^\mu (\partial_\mu + ieA_\mu) + \frac{1-q}{2r} \gamma^r + im \right) \psi = 0. \quad (2.14)$$

For positive-energy solutions, assuming the time-dependence of the eigenfunctions in the form  $e^{-iEt}$  and decomposing the spinor  $\psi$  into the upper ( $\psi_+$ ) and lower ( $\psi_-$ ) components, we find the following equations

$$(E - m)\psi_+ + i \left[ \sigma^l (\partial_l + ieA_l) + \frac{1-q}{2r} \sigma^r \right] \psi_- = 0, \quad (2.15)$$

$$(E + m)\psi_- + i \left[ \sigma^l (\partial_l + ieA_l) + \frac{1-q}{2r} \sigma^r \right] \psi_+ = 0. \quad (2.16)$$

Substituting the function  $\psi_-$  from the second equation into the first one, we obtain the second order differential equation for the spinor  $\psi_+$ :

$$\left[ r^2 \partial_r^2 + r \partial_r + \left( \partial_\phi + ieA_\phi - i \frac{1-q}{2} \sigma^z \right)^2 + r^2 (\partial_z^2 + E^2 - m^2) - \frac{e}{r} \sigma^z \partial_r A_\phi \right] \psi_+ = 0. \quad (2.17)$$

The same equation is obtained for  $\psi_-$ . So, we may say that the general solutions to  $\psi_+$  and  $\psi_-$  can be express in terms of the ansatz below, compatible with the cylindrical symmetry of the physical system,

$$\psi_+ = e^{-ip.x} \begin{pmatrix} R_1(r) e^{iqn_1 \phi} \\ R_2(r) e^{iqn_2 \phi} \end{pmatrix}, \quad (2.18)$$

$$\psi_- = e^{-ip.x} \begin{pmatrix} R_3(r) e^{iqn_1 \phi} \\ R_4(r) e^{iqn_2 \phi} \end{pmatrix}, \quad (2.19)$$

where  $p.x \equiv Et - kz$ .

Imposing that our solutions are eigenfunctions of the total angular momentum along the string,  $J_z$ ,

$$\hat{J}_z \psi = \left( -i \partial_\phi + i \frac{q}{2} \gamma^{(1)} \gamma^{(2)} \right) \psi = qj \psi, \quad (2.20)$$

where

$$j = n + 1/2, \quad n = 0, \pm 1, \pm 2, \dots, \quad (2.21)$$

we obtain that  $n_2 = n_1 + 1$ . From now on we shall use the notations  $n_1 = n$  and  $n_2 = n + 1$ .

In order to construct the complete set of the wave-functions we shall consider, separately, (2.17) in the regions  $r < a$  and  $r > a$ . To the first region, ( $r < a$ ), we have three different configurations of magnetic field already specified by the four-vector potential (2.4)-(2.8). These configurations of the magnetic fields have been used in [24] to analyze the non-relativistic quantum motion of a spin 1/2 charged particle with a gyromagnetic ratio  $g \neq 2$  interacting with

magnetic field and considering the presence of a magnetic dipole interaction; moreover, the corresponding relativistic analysis has been developed in [25]. In the latter, only two configurations of magnetic field have been considered, the homogeneous field and the cylindrical shell with a delta-Dirac distribution.

For the outside region,  $r > a$ , there is no magnetic field and the vector potential given by,

$$A_\phi = -\frac{q\Phi}{2\pi}, \quad (2.22)$$

being  $\Phi$  the magnetic flux. So, the equation (2.17) can be written as following:

$$\left[ r^2 \partial_r^2 + r \partial_r + \left( \partial_\phi + ieA_\phi - i \frac{1-q}{2} \sigma^z \right)^2 + r^2 (\partial_z^2 + E^2 - m^2) \right] \psi_+ = 0. \quad (2.23)$$

Substituting (2.22) into (2.23) we find that the external positive-energy solution of the Dirac equation is given in terms of Bessel,  $J_\mu(z)$ , and Numann,  $Y_\mu(z)$ , functions. A similar result is verified for the lower components of the Dirac spinor. Consequently we can write:

$$\psi^{(+)} = e^{-ip \cdot x} e^{iqn\phi} \begin{pmatrix} C_1 J_{\beta_j}(\lambda r) + D_1 Y_{\beta_j}(\lambda r) \\ [C_2 J_{\beta_j+\epsilon_j}(\lambda r) + D_2 Y_{\beta_j+\epsilon_j}(\lambda r)] e^{iq\phi} \\ A_1 J_{\beta_j}(\lambda r) + B_1 Y_{\beta_j}(\lambda r) \\ [A_2 J_{\beta_j+\epsilon_j}(\lambda r) + B_2 Y_{\beta_j+\epsilon_j}(\lambda r)] e^{iq\phi} \end{pmatrix}, \quad (2.24)$$

with  $n = j - 1/2$  being an integer number. We have defined  $\epsilon_j = 1$  for  $j \geq -\alpha$  and  $\epsilon_j = -1$  for  $j < -\alpha$ , being  $\alpha = eA_\phi/q = -\Phi/\Phi_0$ . Here  $\Phi_0 = 2\pi/e$  is the quantum flux, and

$$\beta_j = q|j + \alpha| - \frac{\epsilon_j}{2}. \quad (2.25)$$

As we can see, we have introduced a set of eight arbitrary constants  $C_i$ ,  $D_i$ ,  $A_i$  and  $B_i$  with  $i = 1, 2$  in the general solution above.

The energy is expressed in terms of  $\lambda$ ,  $k$  and  $m$  by the relation

$$E = \sqrt{\lambda^2 + k^2 + m^2}. \quad (2.26)$$

We can find a relation between the constants of the upper and lower solutions in (2.24) by the use of (2.15) and (2.16). The relations are given by

$$A_1 = \frac{kC_1 - i\epsilon_j \lambda C_2}{E + m}, \quad A_2 = -\frac{kC_2 - i\epsilon_j \lambda C_1}{E + m} \quad (2.27)$$

$$B_1 = \frac{kD_1 - i\epsilon_j \lambda D_2}{E + m}, \quad B_2 = -\frac{kD_2 - i\epsilon_j \lambda D_1}{E + m}. \quad (2.28)$$

In addition, for the further specification of the eigenfunctions, we can impose extra conditions relating the above constants. As such a condition, following [26], we will require the following relations between the upper and lower components:

$$R_3(r) = \rho_s R_1(r), \quad R_4(r) = -\frac{R_2(r)}{\rho_s}, \quad (2.29)$$

with

$$\rho_s = \frac{E + s\sqrt{\lambda^2 + m^2}}{k}, \quad s = \pm 1. \quad (2.30)$$

Doing this we obtain the following relations:

$$A_1 = \rho_s C_1, \quad A_2 = -C_2/\rho_s, \quad (2.31)$$

$$B_1 = \rho_s D_1, \quad B_2 = -D_2/\rho_s. \quad (2.32)$$

Hence, the positive frequency exterior solutions to the Dirac equation, specified by the set of quantum numbers  $\sigma = (\lambda, j, k, s)$ , has the form

$$\psi_{\sigma(out)}^{(+)}(x) = e^{-ip \cdot x} e^{iqn\phi} \begin{pmatrix} C_1 J_{\beta_j}(\lambda r) + D_1 Y_{\beta_j}(\lambda r) \\ i\epsilon_j \rho_s b_s^{(+)} [C_1 J_{\beta_j+\epsilon_j}(\lambda r) + D_1 Y_{\beta_j+\epsilon_j}(\lambda r)] e^{iq\phi} \\ \rho_s [C_1 J_{\beta_j}(\lambda r) + D_1 Y_{\beta_j}(\lambda r)] \\ -i\epsilon_j b_s^{(+)} [C_1 J_{\beta_j+\epsilon_j}(\lambda r) + D_1 Y_{\beta_j+\epsilon_j}(\lambda r)] e^{iq\phi} \end{pmatrix}, \quad (2.33)$$

where we have introduced

$$b_s^{(\pm)} = \frac{\pm m + s\sqrt{\lambda^2 + m^2}}{\lambda}. \quad (2.34)$$

For the region inside,  $r < a$ , we have three different configurations of magnetic field, as we have already mentioned. In this way we have three different solutions for (2.17). Let us represent each radial function by  $R_l^{(i)}$ , where  $i = 1, 2, 3$ , is the index associated with the model and  $l = 1, 2, 3, 4$  the index specifying the the spinor components. By using the general expression for the azimuthal component of the four-vector potential (2.4), we can shown that the relations (2.29) and (2.30) still hold. So, using the relations (2.15) and (2.16) between the upper and lower components of the spinor fields, we can write the inner positive-energy spinor field in the general form below:

$$\psi_{i(in)}^{(+)}(x) = C^{(i)} e^{-ip \cdot x} e^{iqn\phi} \begin{pmatrix} R_1^{(i)}(\lambda, r) \\ i\rho_s b_s^{(+)} R_2^{(i)}(\lambda, r) e^{iq\phi} \\ \rho_s R_1^{(i)}(\lambda, r) \\ -ib_s^{(+)} R_2^{(i)}(\lambda, r) e^{iq\phi} \end{pmatrix}. \quad (2.35)$$

The coefficients  $C_1$  and  $D_1$  in (2.33) and  $C^{(i)}$  in (2.35) are determined from the continuity condition of the fermionic wave function at  $r = a$ . After some intermediate steps we can write,

$$C_1 = -\frac{\pi}{2}(\lambda a) C^{(i)} R_1^{(i)}(\lambda, a) \tilde{Y}_{\beta_j}(\lambda a), \quad (2.36)$$

$$D_1 = \frac{\pi}{2}(\lambda a) C^{(i)} R_1^{(i)}(\lambda, a) \tilde{J}_{\beta_j}(\lambda a), \quad (2.37)$$

where

$$\tilde{Z}_{\beta_j}(z) = \epsilon_j Z_{\beta_j+\epsilon_j}(z) - \mathcal{V}_j^{(i)}(\lambda, a) Z_{\beta_j}(z), \quad \text{with } \mathcal{V}_j^{(i)}(\lambda, a) = \frac{R_2^{(i)}(\lambda, a)}{R_1^{(i)}(\lambda, a)}. \quad (2.38)$$

In (2.38)  $Z_\mu$  represents the Bessel functions  $J_\mu$  or  $Y_\mu$ . With this notation all the informations about the inner structure of the magnetic field is contained in the coefficient  $\mathcal{V}_j^{(i)}$ .

Finally the constant  $C^{(i)}$  can be obtained form the normalization condition,

$$\int d^3x \sqrt{g^{(3)}} \left( \psi_\sigma^{(+)} \right)^\dagger \psi_{\sigma'}^{(+)} = \delta_{\sigma, \sigma'}, \quad (2.39)$$

where delta symbol on the right-hand side is understood as the Dirac delta function for continuous quantum numbers  $\lambda$  and  $k$ , and the Kronecker delta for discrete ones  $n$  and  $s$ , and  $g^{(3)}$  is the determinant of the spatial metric tensor. The integral over the radial coordinate should be

done in the interval  $[0, \infty)$ . Due to cylindrical symmetry of this system we can write the spinor field in a general form as shown bellow:

$$\psi_{\sigma}^{(+)}(x) = e^{-ip \cdot x} e^{iqn\phi} \begin{pmatrix} F_1(\lambda, r) \\ i\rho_s b_s^{(+)} F_2(\lambda, r) e^{iq\phi} \\ \rho_s F_1(\lambda, r) \\ -ib_s^{(+)} F_2(\lambda, r) e^{iq\phi} \end{pmatrix}. \quad (2.40)$$

Consequently from (2.39) we obtain,

$$(1 + \rho_s^2) \left[ \int_0^{\infty} dr \, r F_1^*(\lambda, r) F_1(\lambda', r) + (b_s^{(+)})^2 \int_0^{\infty} dr \, r F_2^*(\lambda, r) F_2(\lambda', r) \right] = \frac{q}{(2\pi)^2} \delta(\lambda - \lambda'). \quad (2.41)$$

The integral over the interior region is finite, consequently the dominant contribution in (2.41) for  $\lambda' = \lambda$  comes from the integration in the exterior region. By using the standard integrals involving the cylindrical Bessel functions, we find

$$(2\pi)^2 [|C_1|^2 + |D_1|^2] = \frac{q\lambda}{(1 + \rho_s^2)(1 + (b_s^{(+)})^2)}. \quad (2.42)$$

Substituting (2.36) and (2.37) into the above equation we find:

$$C^{(i)} R_1^{(i)}(\lambda, a) = \Xi(\lambda, a), \quad (2.43)$$

with

$$\Xi(\lambda, a) = \frac{1}{a\pi^2} \left[ \frac{q}{\lambda} \frac{1}{(1 + \rho_s^2)} \frac{1}{(1 + (b_s^{(+)})^2)} \right]^{1/2} \frac{1}{\sqrt{(\tilde{Y}_{\beta_j}(\lambda a))^2 + (\tilde{J}_{\beta_j}(\lambda a))^2}}. \quad (2.44)$$

This relation determines the normalization constant for the interior wave function. With this normalization we can construct the spinor function for the external region,  $r > a$ :

$$\psi_{\sigma(out)}^{(+)}(x) = N^{(+)} e^{-ip \cdot x} e^{iqn\phi} \begin{pmatrix} g_{\beta_j}(\lambda a, \lambda r) , \\ i\epsilon_j \rho_s b_s^{(+)} g_{\beta_j + \epsilon_j}(\lambda a, \lambda r) e^{iq\phi} \\ \rho_s g_{\beta_j}(\lambda a, \lambda r) \\ -i\epsilon_j b_s^{(+)} g_{\beta_j + \epsilon_j}(\lambda a, \lambda r) e^{iq\phi} \end{pmatrix}, \quad (2.45)$$

where we have introduced the notations,

$$N^{(+)} = \frac{1}{2\pi} \left[ \frac{q\lambda}{(1 + \rho_s^2) (1 + (b_s^{(+)})^2)} \right]^{1/2}, \quad (2.46)$$

$$g_{\beta_j}(\lambda a, \lambda r) = \frac{\tilde{Y}_{\beta_j}(\lambda a) J_{\beta_j}(\lambda r) - \tilde{J}_{\beta_j}(\lambda a) Y_{\beta_j}(\lambda r)}{\sqrt{(\tilde{Y}_{\beta_j}(\lambda a))^2 + (\tilde{J}_{\beta_j}(\lambda a))^2}} \quad (2.47)$$

and

$$g_{\beta_j + \epsilon_j}(\lambda a, \lambda r) = \frac{\tilde{Y}_{\beta_j}(\lambda a) J_{\beta_j + \epsilon_j}(\lambda r) - \tilde{J}_{\beta_j}(\lambda a) Y_{\beta_j + \epsilon_j}(\lambda r)}{\sqrt{(\tilde{Y}_{\beta_j}(\lambda a))^2 + (\tilde{J}_{\beta_j}(\lambda a))^2}}. \quad (2.48)$$

The out-side negative-energy fermionic wave-function can be obtained in a similar way, or by the charge conjugation operator,  $\psi_{\sigma}^{(-)} = i\gamma^{(2)}\hat{K}\psi_{\sigma}^{(+)}$ , where  $\hat{K}$  is the complex conjugation operator [27]. The corresponding result is given by the expression:

$$\psi_{\sigma(out)}^{(-)}(x) = N^{(-)} e^{ip \cdot x} e^{-iq(n+1)\phi} \begin{pmatrix} g_{\beta_j+\epsilon_j}(\lambda a, \lambda r) \\ i\epsilon_j \rho_s b_s^{(-)} g_{\beta_j}(\lambda a, \lambda r) e^{iq\phi} \\ \rho_s g_{\beta_j+\epsilon_j}(\lambda a, \lambda r) \\ -i\epsilon_j b_s^{(-)} g_{\beta_j}(\lambda a, \lambda r) e^{iq\phi} \end{pmatrix}, \quad (2.49)$$

where the phase  $i\epsilon_j$  was absorbed into the normalization constant and have used  $b_s^{(-)} = 1/b_s^{(+)}$ . The normalization constant becomes,

$$N^{(-)} = (N^{(+)})^{\dagger} b_s^{(+)} = \frac{1}{2\pi} \left[ \frac{q\lambda}{(1 + \rho_s^2)(1 + (b_s^{(-)})^2)} \right]^{1/2}. \quad (2.50)$$

Having the negative-energy wave-function for the region outside the magnetic flux, i.e., for  $r > a$ , we can use it for the investigation of the vacuum fermionic current densities.

### 3 Fermionic current

Here we shall evaluate the vacuum expectation value (VEV) of the fermionic current density operator,  $j^{\mu} = e\bar{\psi}\gamma^{\mu}\psi$ , by using the mode sum formula,

$$\langle j^{\mu}(x) \rangle = e \sum_{\sigma} \bar{\psi}_{\sigma}^{(-)}(x) \gamma^{\mu} \psi_{\sigma}^{(-)}(x), \quad (3.1)$$

where we are using the compact notation defined by

$$\sum_{\sigma} = \int_0^{\infty} d\lambda \int_{-\infty}^{+\infty} dk \sum_{j=\pm 1/2, \dots} \sum_{s=\pm 1}. \quad (3.2)$$

In the following subsections we shall calculate separately all the components of the VEV of the fermionic current densities.

#### 3.1 Charge and radial current densities

Let us start the calculation of the charge density,

$$\rho(x) = \langle j^0(x) \rangle = e \sum_{\sigma} (\psi_{\sigma}^{(-)}(x))^{\dagger} \psi_{\sigma}^{(-)}(x). \quad (3.3)$$

Substituting (2.49) and (2.50) into (3.3) we obtain

$$\rho(x) = \frac{eq}{(2\pi)^2} \int_{-\infty}^{\infty} dk \int_0^{\infty} d\lambda \sum_{j=\pm 1/2, \dots} ((g_{\beta_j}(\lambda a, \lambda r))^2 + (g_{\beta_j+\epsilon_j}(\lambda a, \lambda r))^2). \quad (3.4)$$

Moreover, substituting (2.47) and (2.48) into the above expression, and after some intermediate steps, we obtain,

$$\rho(r) = \rho_s(r) + \rho_c(r), \quad (3.5)$$

where

$$\rho_s(r) = \frac{eq}{(2\pi)^2} \int_{-\infty}^{\infty} dk \sum_{j=\pm 1/2, \dots} \int_0^{\infty} d\lambda \lambda \left( J_{\beta_j}^2(\lambda r) + J_{\beta_j+\epsilon_j}^2(\lambda r) \right) \quad (3.6)$$

represents the charge density in a cosmic string spacetime carrying a zero-thickness magnetic flux along its axis, and

$$\rho_c(r) = -\frac{eq}{2(2\pi)^2} \int_{-\infty}^{\infty} dk \sum_j \int_0^{\infty} d\lambda \lambda \tilde{J}_{\beta_j}(\lambda a) \sum_{l=1}^2 \frac{(H_{\beta_j}^{(l)}(\lambda r))^2 + (H_{\beta_j+\epsilon_j}^{(l)}(\lambda r))^2}{\tilde{H}_{\beta_j}^{(l)}(\lambda a)}, \quad (3.7)$$

is the charge density induced by the magnetic flux tube around the string. In (3.7)  $H_{\nu}^{(l)}(x)$  with  $l = 1, 2$  are the Hankel functions.

In [28] the charge density,  $\rho_s$ , was analyzed. There it was shown that the integrations over  $\lambda$  and  $k$  in (3.6) are divergent. In order to obtain a finite and well defined result we introduced a cutoff function. With this cutoff function the integrals could be evaluated. By subtracting the Minkowskian part, which corresponds to subtract  $\alpha_0 = 0$  and  $q = 1$  contribution in the result, the cutoff function can be removed and a vanishing result was found for the renormalized charge density.

As to  $\rho_c$ , in principle it is finite and does not require any regularization procedure. To evaluate this contribution we proceed as follows: in the complex  $\lambda$  plane we rotate the integration contour by the angle  $\pi/2$  for  $l = 1$  and by the angle  $-\pi/2$  for  $l = 2$ . Moreover, it is shown in Appendix A that the coefficient  $\mathcal{V}_j^{(i)}(\lambda, a)$  in (2.38) satisfy the relation below:<sup>2</sup>

$$\mathcal{V}_j^{(i)}(\pm i\lambda, a) = \pm i \text{Im}\{\mathcal{V}_j^{(i)}(i\lambda, a)\}. \quad (3.8)$$

So, by using (3.8) and the well known relations involving the Bessel and Hankel functions of imaginary argument with the modified Bessel functions [29], we can see that the integrand of the first contribution ( $l = 1$ ) cancels the other from the second contribution ( $l = 2$ ), providing a vanishing result for (3.7). So, we conclude that there is no induced charge density for this system.

To analyze the VEV of the radial and axial current densities, we use the sum mode below,

$$\langle j^r(x) \rangle = e \sum_{\sigma} (\psi_{\sigma}^{(-)}(x))^{\dagger} \gamma^0 \gamma^r \psi_{\sigma}^{(-)}(x) \quad (3.9)$$

and

$$\langle j^z(x) \rangle = e \sum_{\sigma} (\psi_{\sigma}^{(-)}(x))^{\dagger} \gamma^0 \gamma^z \psi_{\sigma}^{(-)}(x). \quad (3.10)$$

Substituting (2.49) and (2.50) into the above expressions we observe that: For the radial current density there is a direct cancellations between all terms involved. As to the axial current the result obtained is an odd function of the variable  $k$ , consequently integrating over this variable a vanishing result is promptly obtained. This latter result is in agreement with the boost symmetry along the  $z$ -direction of the system. So, we conclude that there are no induced radial or axial current densities in this system.

### 3.2 Azimuthal current density

The VEV of the azimuthal current density is given by,

$$\langle j^{\phi}(x) \rangle = e \sum_{\sigma} (\psi_{\sigma}^{(-)}(x))^{\dagger} \gamma^0 \gamma^{\phi} \psi_{\sigma}^{(-)}(x). \quad (3.11)$$

---

<sup>2</sup> In fact the relation (3.8) is satisfied for all radial functions associated with the three configurations of magnetic field.

By using (2.49) and (2.50) and the explicit form of the Dirac matrices given by (2.11) and (2.12) the following expression below is obtained:

$$\langle j^\phi \rangle = \frac{eq}{2\pi^2 r} \sum_{\sigma} \frac{\epsilon_j b_s^{(-)} (\rho_s^2 - 1) \lambda}{(1 + (b_s^{(-)})^2)(1 + \rho_s^2)} g_{\beta_j}(\lambda a, \lambda r) g_{\beta_j + \epsilon_j}(\lambda r, \lambda r) . \quad (3.12)$$

We can easily see that

$$\frac{b_s^{(-)} (\rho_s^2 - 1)}{(1 + (b_s^{(-)})^2)(1 + \rho_s^2)} = \frac{\lambda}{2\sqrt{\lambda^2 + k^2 + m^2}} . \quad (3.13)$$

So, substituting this expression into (3.12), we can see that the summation over  $s$  provides a factor 2. So, it remains only the expression below,

$$\langle j^\phi \rangle = \frac{eq}{2\pi^2 r} \int_{-\infty}^{\infty} dk \int_0^{\infty} \frac{\lambda^2 d\lambda}{\sqrt{\lambda^2 + k^2 + m^2}} \sum_j \epsilon_j g_{\beta_j}(\lambda a, \lambda r) g_{\beta_j + \epsilon_j}(\lambda a, \lambda r) . \quad (3.14)$$

Developing the product of  $g_{\beta_j}(\lambda a, \lambda r) g_{\beta_j + \epsilon_j}(\lambda a, \lambda r)$  in a convenient form, i.e., separating the contributions that does not depend on the inner structure of the magnetic field from the other that does, we can written the above result as the sum of two terms as shown below:

$$\langle j^\phi(x) \rangle = \langle j^\phi(x) \rangle_s + \langle j^\phi(x) \rangle_c . \quad (3.15)$$

The first term,  $\langle j^\phi(x) \rangle_s$ , corresponds to the azimuthal current density in the geometry of a straight cosmic having a magnetic flux running along its core, and the second,  $\langle j^\phi(x) \rangle_c$ , is induced by the magnetic tube of radius  $a$ .

At this point we would like to analyze separately both contributions.

### 3.2.1 Azimuthal current induced by a zero-thickness magnetic flux

The azimuthal current induced by a magnetic flux running along the idealized cosmic string is given by,

$$\langle j^\phi(x) \rangle_s = \frac{eq}{2\pi^2 r} \int_{-\infty}^{\infty} dk \int_0^{\infty} \frac{d\lambda \lambda^2}{\sqrt{\lambda^2 + k^2 + m^2}} \sum_j \epsilon_j J_{\beta_j}(\lambda r) J_{\beta_j + \epsilon_j}(\lambda r) . \quad (3.16)$$

The explicit calculation of this contribution was given in [28]. Here we briefly review its more important results. Using the identity below,

$$\frac{1}{\sqrt{m^2 + k^2 + \lambda^2}} = \frac{2}{\sqrt{\pi}} \int_0^{\infty} dt e^{-(m^2 + k^2 + \lambda^2)t^2} , \quad (3.17)$$

into (3.16), it is possible to integrate over the variable  $\lambda$  by using the results form [30]:

$$\int_0^{\infty} d\lambda \lambda^2 e^{-\lambda^2 t^2} J_{\beta_j}(\lambda r) J_{\beta_j + \epsilon_j}(\lambda r) = \frac{e^{-r^2/(2t^2)}}{4t^4} r \epsilon_j [I_{\beta_j}(r^2/(2t^2)) - I_{\beta_j + \epsilon_j}(r^2/(2t^2))] . \quad (3.18)$$

Introducing a new variable  $y = r^2/(2t^2)$ , we get

$$\langle j^\phi \rangle_s = \frac{eq}{2\pi^2 r^4} \int_0^{\infty} dy y e^{-y - m^2 r^2/(2y)} [\mathcal{I}(q, \alpha_0, y) - \mathcal{I}(q, -\alpha_0, y)] , \quad (3.19)$$

where  $\mathcal{I}(q, \alpha_0, y)$  is defined by

$$\mathcal{I}(q, \alpha_0, z) = \sum_j I_{\beta_j}(z) = \sum_{n=0}^{\infty} [I_{q(n+\alpha_0+1/2)-1/2}(z) + I_{q(n-\alpha_0+1/2)+1/2}(z)] , \quad (3.20)$$

and

$$\sum_j I_{\beta_j + \epsilon_j}(z) = \mathcal{I}(q, -\alpha_0, z) . \quad (3.21)$$

In the above development, we have used the notation

$$\alpha = eA_\phi/q = -\Phi/\Phi_0 = n_0 + \alpha_0 , \quad (3.22)$$

with  $n_0$  being an integer number. So we conclude that (3.19) is an odd function of  $\alpha_0$ .

In [31] we have presented an integral representation for  $\mathcal{I}(q, \alpha_0, y)$ :

$$\begin{aligned} \mathcal{I}(q, \alpha_0, z) &= \frac{e^z}{q} - \frac{1}{\pi} \int_0^\infty dy \frac{e^{-z \cosh y} f(q, \alpha_0, y)}{\cosh(qy) - \cos(q\pi)} \\ &\quad + \frac{2}{q} \sum_{k=1}^p (-1)^k \cos[2\pi k(\alpha_0 - 1/2q)] e^{z \cos(2\pi k/q)} , \end{aligned} \quad (3.23)$$

with  $2p < q < 2p + 2$  and with the notation

$$\begin{aligned} f(q, \alpha_0, y) &= \cos[q\pi(1/2 - \alpha_0)] \cosh[(q\alpha_0 + q/2 - 1/2)y] \\ &\quad - \cos[q\pi(1/2 + \alpha_0)] \cosh[(q\alpha_0 - q/2 - 1/2)y] . \end{aligned} \quad (3.24)$$

For  $1 \leq q < 2$ , the last term on the right-hand side of Eq. (3.23) is absent.

By using the result (3.23), and after the integration over  $y$ , the expression (3.19) is presented in the form

$$\begin{aligned} \langle j^\phi \rangle_s &= \frac{em^2}{\pi^2 r^2} \left[ \sum_{k=1}^p \frac{(-1)^k}{\sin(\pi k/q)} \sin(2\pi k\alpha_0) K_2(2mr \sin(\pi k/q)) \right. \\ &\quad \left. + \frac{q}{\pi} \int_0^\infty dy \frac{g(q, \alpha_0, 2y) K_2(2mr \cosh y)}{[\cosh(2qy) - \cos(q\pi)] \cosh y} \right] . \end{aligned} \quad (3.25)$$

In the above expression  $K_\nu(x)$  is the Macdonald function, and

$$\begin{aligned} g(q, \alpha_0, y) &= \cos[q\pi(1/2 + \alpha_0)] \cosh[q(1/2 - \alpha_0)y] \\ &\quad - \cos[q\pi(1/2 - \alpha_0)] \cosh[q(1/2 + \alpha_0)y] . \end{aligned} \quad (3.26)$$

As we can see  $\langle j^\phi \rangle_s$  depends only on  $\alpha_0$ , and vanishes for the case where this parameter is zero

### 3.2.2 Core-induced azimuthal current

As to  $\langle j^\phi(x) \rangle_c$ , we can show that it can be written by,

$$\begin{aligned} \langle j^\phi(x) \rangle_c &= -\frac{eq}{(2\pi)^2 r} \int_{-\infty}^\infty dk \int_0^\infty \frac{d\lambda \lambda^2}{\sqrt{\lambda^2 + k^2 + m^2}} \\ &\quad \times \sum_j \epsilon_j \tilde{J}_{\beta_j}(\lambda a) \sum_{l=1}^2 \frac{H_{\beta_j}^{(l)}(\lambda r) H_{\beta_j + \epsilon_j}^{(l)}(\lambda r)}{\tilde{H}_{\beta_j}^{(l)}(\lambda a)} . \end{aligned} \quad (3.27)$$

In order to develop this calculation, we rotate the integrals contour in the complex plane  $\lambda$  as follows: by the angle  $\pi/2$  for  $l = 1$  and  $-\pi/2$  for  $l = 2$ . By using the property (3.8), one can see that the integral over the segments  $(0, i\sqrt{m^2 + k^2})$  and  $(0, -i\sqrt{m^2 + k^2})$  are canceled. In the remaining integral over the imaginary axis we introduce the modified Bessel functions.

Moreover, writing imaginary integral variable by  $\lambda = \pm iz$ , the core-induced azimuthal current reads,

$$\langle j^\phi(x) \rangle_c = \frac{eq}{\pi^3 r} \int_0^\infty dk \int_{\sqrt{k^2+m^2}}^\infty \frac{dz z^2}{\sqrt{z^2 - k^2 - m^2}} \sum_j K_{\beta_j}(zr) K_{\beta_j+\epsilon_j}(zr) F_j^{(i)}(za) , \quad (3.28)$$

where we use the notation

$$F_j^{(i)}(y) = \frac{I_{\beta_j+\epsilon_j}(y) - \text{Im}[\mathcal{V}_j^{(i)}(iy/a, a)] I_{\beta_j}(y)}{K_{\beta_j+\epsilon_j}(y) + \text{Im}[\mathcal{V}_j^{(i)}(iy/a, a)] K_{\beta_j}(y)} . \quad (3.29)$$

After a convenient coordinate transformations we write (3.28) as follow:

$$\langle j^\phi(x) \rangle_c = \frac{eq}{\pi^2 r^4} \int_{mr}^\infty z^2 dz \sum_j K_{\beta_j}(z) K_{\beta_j+\epsilon_j}(z) F_j^{(i)}(z(a/r)) . \quad (3.30)$$

Before to start explicit numerical analysis related to the core-induced azimuthal current, let us now evaluate the behavior of it at large distance from the core. First we consider the massive fields and in the limit  $mr \gg 1$ . In order to develop this analysis, we assume that the product  $K_{\beta_j}(z) K_{\beta_j+\epsilon_j}(z)$  can be expressed in terms of their corresponding asymptotic forms. So we have the induced current density given below

$$\langle j^\phi \rangle_c \approx \frac{eq}{2\pi r^4} \int_{mr}^\infty dz z e^{-2z} \sum_j F_j^{(i)}(z(a/r)) . \quad (3.31)$$

The dominant contribution is given from the region near the lower limit of integration. Then the leading order contribution is,

$$\langle j^\phi(r) \rangle_c \approx \frac{eqm^4}{4\pi(mr)^3} e^{-2mr} \sum_j F_j^{(i)}(ma) . \quad (3.32)$$

So, we can see that for massive fields and at large distances from the core, the core-induced azimuthal current decays with  $e^{-2mr}/(mr)^3$ . Comparing this behavior with the corresponding one for the zero-thickness azimuthal current,  $\langle j_\phi \rangle_c$ , given by Eq. (3.25), we observe in [28] that for  $q > 2$  the latter decays with  $e^{-2mr \sin(\pi/q)}/(mr)^{5/2}$ , consequently dominates the total azimuthal current. For  $q \leq 2$ , the contributions of  $\langle j_\phi \rangle_s$  and  $\langle j_\phi \rangle_c$  to the total azimuthal current, at large distances, are of the same order.

Our next analysis will be developed by using explicitly the radial functions in the region inside the tube. In appendix A we provide exact solutions for  $R_1(r)$  and  $R_2(r)$  for the three different configurations of magnetic field. They are:

1. For the cylindrical shell:

$$\begin{aligned} R_1^{(1)}(r) &= J_{\nu_j}(\lambda r) \\ R_2^{(1)}(r) &= \hat{\epsilon}_j J_{\nu_j+\hat{\epsilon}_j}(\lambda r) , \end{aligned} \quad (3.33)$$

where  $\nu_j = q|j| - \frac{\tilde{\epsilon}_j}{2}$ , with  $\tilde{\epsilon}_j = 1$  for  $j > 0$  and  $\tilde{\epsilon}_j = -1$  for  $j < 0$ .

2. For the magnetic field proportional to  $1/r$ :

$$\begin{aligned} R_1^{(2)}(r) &= \frac{M_{\kappa, \nu_j}(\xi r)}{\sqrt{r}} \\ R_2^{(2)}(r) &= C_j^{(2)} \frac{M_{\kappa, \nu_j + \hat{\epsilon}_j}(\xi r)}{\sqrt{r}}, \end{aligned} \quad (3.34)$$

where

$$\xi = \frac{2}{a} \sqrt{q^2 \alpha^2 - \lambda^2 a^2}, \quad \kappa = -\frac{2q^2 j \alpha}{\xi a} \quad (3.35)$$

and

$$C_j^{(2)} = \begin{cases} \frac{\lambda}{\xi} \frac{1}{(2q|j|+1)}, & j > 0. \\ -\frac{\xi}{\lambda} (2q|j|+1), & j < 0. \end{cases} \quad (3.36)$$

3. For the homogeneous magnetic field:

$$\begin{aligned} R_1^{(3)}(r) &= \frac{M_{\kappa - \frac{1}{4}, \frac{\nu_j}{2}}(\tau r^2)}{r} \\ R_2^{(3)}(r) &= C_j^{(3)} \frac{M_{\kappa + \frac{1}{4}, \frac{\nu_j + \hat{\epsilon}_j}{2}}(\tau r^2)}{r}, \end{aligned} \quad (3.37)$$

where  $\tau$  and  $\kappa$  are given by where  $\tau$  and  $\kappa$  are given by

$$\tau = q\alpha/a^2, \quad \kappa = \frac{\lambda^2}{4\tau} - \frac{qj}{2}, \quad (3.38)$$

with

$$C_j^{(3)} = \begin{cases} \frac{\lambda}{\sqrt{\tau}} \frac{1}{2q|j|+1} & j > 0. \\ -\frac{\sqrt{\tau}}{\lambda} (2q|j|+1), & j < 0. \end{cases} \quad (3.39)$$

For the second and third models, the radial functions are given in terms of Whittaker functions,  $M_{\kappa, \nu}(z)$ .

For massless fields and at large distance from the core, the behavior of the core-induced azimuthal current can be developed as follows: instead to use the summation on the angular moment  $j$  in (3.30), we use  $n = j - 1/2$ . In this way, we shall use a new notation,  $F_n^{(i)} \equiv F_j^{(i)}$ . Moreover, we change  $n$  by  $n - n_0$ , being  $n_0$  given in (3.22). So from (3.30) we can write,

$$\langle j^\phi(x) \rangle_c = \frac{eq}{\pi^2 r^4} \int_0^\infty dz z^2 \sum_{n=-\infty}^\infty K_\beta(z) K_{\tilde{\beta}}(z) F_{n-n_0}^{(i)}(z(a/r)). \quad (3.40)$$

In the above expression we are using the notation:

$$F_{n-n_0}^{(i)}(z(a/r)) = \frac{I_{\tilde{\beta}}(z(a/r)) - \text{Im}[\mathcal{V}_{n-n_0}^{(i)}(iz, (a/r))] I_\beta(z(a/r))}{K_{\tilde{\beta}}(z(a/r)) + \text{Im}[\mathcal{V}_{n-n_0}^{(i)}(iz, (a/r))] K_\beta(z(a/r))}. \quad (3.41)$$

In (3.41) the orders of Bessel functions are given by

$$\begin{aligned} \beta &= q|n + 1/2 + \alpha_0| - \frac{1}{2} \frac{|n + 1/2 + n_0|}{n + 1/2 + \alpha_0}, \\ \tilde{\beta} &= q|n + 1/2 + \alpha_0| + \frac{1}{2} \frac{|n + 1/2 + n_0|}{n + 1/2 + \alpha_0}. \end{aligned} \quad (3.42)$$

Expanding the integrand of (3.40) in powers of  $a/r$ , the dominant term is given by the smaller power of this ratio. So we have two possibilities: for  $\alpha_0 > 0$  ( $0 \leq \alpha_0 < 1/2$ ) this term is given by  $n = -1$ , and for  $\alpha_0 < 0$  ( $-1/2 < \alpha_0 \leq 0$ ) this term is given for  $n = 0$ .

Now, using the expansions for the modified Bessel functions for small arguments [29], the leader contributions are:

- For  $\alpha_0 > 0$ :

$$F_{-1-n_0}^{(i)}\left(z\frac{a}{r}\right) \approx \frac{2}{\Gamma^2(\beta)} \frac{1 + i\mathcal{V}_{-1-n_0}^{(i)}(iz, a/r) \left(z\frac{a}{r}\right) \left(\frac{az}{2r\beta}\right)}{\frac{\Gamma(1-\beta)}{\Gamma(\beta)} - i\mathcal{V}_{-1-n_0}^{(i)}(iz, a/r) \left(z\frac{R}{r}\right) \left(\frac{az}{2r}\right) \left(\frac{2r}{az}\right)^{2\beta}}. \quad (3.43)$$

- For  $\alpha_0 < 0$ , and

$$F_{-n_0}^{(i)}\left(z\frac{a}{r}\right) \approx -\frac{2}{\beta\Gamma^2(\beta)} \frac{1 + i\mathcal{V}_{-n_0}^{(i)}(iz, a/r) \left(z\frac{R}{r}\right) \left(\frac{2r\beta}{az}\right)}{\left(\frac{2r}{az}\right)^{2\beta} - i\frac{\Gamma(1-\beta)}{\Gamma(\beta)}\mathcal{V}_{-n_0}^{(i)}(iz, a/r) \left(z\frac{R}{r}\right) \left(\frac{2r}{az}\right)}. \quad (3.44)$$

The next steps are the calculations of the dominants contribution for the coefficient that contains all the information about the core,  $\mathcal{V}_{-1-n_0}^{(i)}(iz, a/r)$  and  $\mathcal{V}_{-n_0}^{(i)}(iz, a/r)$ , for the three models. This can be done by explicit substitution of the radial functions,  $R_1^{(i)}(iz, a/r)$  and  $R_2^{(i)}(iz, a/r)$ , into (2.38). So, for massless fields, we find:

$$\langle j^\phi(r) \rangle_c \approx -2 \frac{|\alpha_0|}{\alpha_0} \frac{eq}{\pi^2 r^4} \frac{\beta - \chi^{(l)}}{\left(\frac{2r}{a}\right)^{2\beta} \chi^{(l)}} \frac{\beta}{2\beta + 1}, \quad (3.45)$$

where

$$\beta = q \left( \frac{1}{2} - |\alpha_0| \right) + \frac{1}{2} \quad (3.46)$$

and  $\chi^{(l)}$  is a parameter depending on the specific model adopted for the magnetic field, given bellow by:

$$\chi^{(l)} = \begin{cases} \nu = q|n_0 - \frac{1}{2} \frac{|\alpha_0|}{\alpha_0}| - \frac{1}{2} \frac{|\alpha_0|}{\alpha_0}, & \text{for the model (i)} \\ q\alpha(q+1) \frac{M_{\frac{q}{2} \frac{|\alpha_0|}{\alpha_0}, \nu}^{(2q\alpha)}}{M_{\frac{q}{2} \frac{|\alpha_0|}{\alpha_0}, \nu+1}^{(2q\alpha)}}, & \text{for the model (ii)} \\ \frac{\sqrt{q\alpha}}{2}(q+1) \frac{M_{-\frac{1}{2} \frac{|\alpha_0|}{\alpha_0} \frac{q+1}{2}, \frac{\nu}{2}}^{(\tau R^2)}}{M_{-\frac{1}{2} \frac{|\alpha_0|}{\alpha_0} \frac{q+1}{2}, \frac{\nu}{2}}^{(\tau R^2)}}, & \text{for the model (iii)}. \end{cases} \quad (3.47)$$

On basis of this results we can say that for the three models considered, the core-induced azimuthal current density decays with,  $\frac{1}{r^4(a/r)^{2\beta}}$ , for large distance from the tube. We have shown in [28] that the massless limit of the zero-thickness azimuthal current given in (3.25), decays with  $1/r^4$ . So, we conclude that for large distance from the core, the total azimuthal current, (3.15), is dominated by the zero-thickness contribution.

Now let us investigate the behavior of the core-induced azimuthal current density near the core, for the three models. In general the current diverges in this region. The dominant contribution in (3.30) comes from the contribution of large  $|j|$ . To find the leading term it is convenient to introduce a new variable  $z = \beta_j x$ , and use the uniform expansion for large order for the modified Bessel functions [29]. However, before to do that, we would like to notice that, changing  $n \rightarrow -n - 1$  the summation over  $j$  keeps unchanged, but the parameter  $\nu_j$  change as  $\nu_j \rightarrow \tilde{\nu}_j$  and  $\tilde{\nu}_j \rightarrow \nu_j$ . If, in addition, we also change  $\alpha \rightarrow -\alpha$ , then  $\beta_j \rightarrow \tilde{\beta}_j$  and  $\tilde{\beta}_j \rightarrow \beta_j$ . It means that, when we make  $n \rightarrow -n - 1$  and  $\alpha \rightarrow -\alpha$  we have  $F_j^{(i)}(y) \rightarrow -F_j^{(i)}(y)$ . On basis

of this analysis, and considering  $\alpha > 0$ , the behavior of the core-induced azimuthal current near the boundary is given by,

$$\langle j^\phi(x) \rangle_c \approx -2 \frac{eq}{\pi^2 r^4} \sum_{n>0} \beta_j^3 \int_{\frac{mr}{\beta_j}}^{\infty} dx x^2 F_j^{(i)}(\beta_j x(a/r)) K_{\beta_j}(\beta_j x) K_{\beta_j + \epsilon_j}(\beta_j x) . \quad (3.48)$$

Because we are considering  $n \gg 1$ , from now on we use the approximation,  $\beta_j \approx \nu_j \approx qn$ .

For the three models, it is necessary to find the leading term of  $F_j^{(i)}$  for large value of  $j$ . For the first two models, this term is obtained by using the uniform expansion for large order for the modified Bessel functions for the first model and the asymptotic expansion for the corresponding Whittaker functions for the second model. After some intermediate and long steps, we found that both leading terms coincide and are given below,

$$F_j^{(1,2)}(qn x(a/r)) \approx \frac{1}{4q^2 \pi} \frac{e^{2qn\tilde{\eta}}}{n^2(1 + e^{2\tilde{\eta}})} , \quad (3.49)$$

where  $\tilde{\eta} = \sqrt{1 + x^2(a/r)^2}$ . The third model converge to the same result. In order to see that we express the Whittaker function in terms of the confluent hypergeometric functions [29],  $M_{\kappa, \mu}(z) = e^{-z/2} z^{1/2+\mu} M(1/2 + \mu - \kappa, 1 + 2\mu; z)$ , and use the expansion below for the latter,

$$M(a, b; z) = \Gamma(b) e^{zx} \sum_{k=0}^{\infty} C_k z^k (-az)^{\frac{1}{2}(1-b-k)} J_{b-1+k}(2\sqrt{-az}) . \quad (3.50)$$

Finally we use the uniform expansion for large order for the Bessel function. So, for the three models, the core-induced azimuthal current density is given by

$$\langle j^\phi(x) \rangle_c \approx -\frac{eq}{4\pi^2 r^4} \sum_{n>0} \int_{\frac{mr}{qn}}^{\infty} dz z^2 \frac{e^{-2qn(\eta - \tilde{\eta})}}{(1 + e^{2\tilde{\eta}}) \sqrt{1 + z^2}} , \quad (3.51)$$

where  $\eta = \sqrt{1 + x^2}$ . Using the approximation  $\eta - \tilde{\eta} \approx z(1 - a/r)$ , and observing that the denominator of the integrand in (3.51) can be approximate to unity, for the three models, we have:

$$\langle j^\phi(x) \rangle_c \approx -\frac{eq}{4\pi^2 r^4} \sum_{n>0} \int_{\frac{mr}{qn}}^{\infty} dz z^2 e^{-2qn(1-a/r)} . \quad (3.52)$$

Solving the above integral we have

$$\langle j^\phi(r) \rangle_c \approx -\frac{e}{(4\pi q)^2} \frac{1}{r} \frac{1}{(r-a)^3} . \quad (3.53)$$

Here, we must notice that the current density diverges near the boundary.

Because the zero-thickness azimuthal current,  $\langle j^\phi(r) \rangle_s$ , presents a finite value near the boundary, we can conclude that, in this region, the total azimuthal current, (3.15) is dominated by the core-induced contribution.

An alternative way to show that the three models provide the same result for the core-induced azimuthal current near the boundary, is given by analyzing the radial differential equations (A.1) and (A.2) given in Appendix A for large value of  $j$ . Replacing the parameter  $\lambda$  by  $i\nu_j z$ , specifically for (A.1), we get:<sup>3</sup>

$$r^2 R_1''(r) + r R_1'(r) - r^2 \nu_j^2 z^2 R_1(r) - \nu_j^2 \left( 1 + \frac{2eA_\phi(r)}{\nu_j} \right) R_1(r) \approx 0 . \quad (3.54)$$

---

<sup>3</sup>For  $R_2(r)$  the equation is similar to (3.54) by changing  $\nu_j$  by  $\nu_j + \frac{\epsilon_j}{2}$ .

Substituting (A.3), (A.11) or (A.24) into the above equation, it is possible to see that the solutions can be written in a general form below:

$$R_1(r) = I_{\nu_j}(\nu_j z r) f(r) , \quad (3.55)$$

where  $f(r)$  is equal to unity for the first model, Eq. (A.3), and for the second and third models, it reads,

$$f(r) \approx 1 - \frac{r q \alpha}{a} + \frac{q \alpha z}{2} \left( \frac{q \alpha}{a z} + 1 \right) \frac{r^2}{a} + O(\nu_j^{-1}) \quad (3.56)$$

and

$$f(r) \approx e^{-\frac{r q \alpha}{a^2 z}} \left( 1 + \frac{r q \alpha}{a^2 z} - \frac{q \alpha}{2} \left( 1 - \frac{q \alpha}{z^2 a^2} \right) \frac{r^2}{a^2} + O(\nu_j^{-1}) \right) , \quad (3.57)$$

respectively.

Because the coefficient  $\mathcal{V}_j^{(i)}$  depends on the ratio of the two radial functions,  $R_2(r)$  and  $R_1(r)$ , for large value of  $j$ , the leading term of this ration is:

$$\frac{R_2(r)}{R_1(r)} \approx \frac{I_{\nu_j + \tilde{\epsilon}_j/2}((\nu_j + \tilde{\epsilon}_j/2) z r)}{I_{\nu_j}(\nu_j z r)} . \quad (3.58)$$

Consequently the three models behave, in this limit, in a similar way.

After these above general descriptions of the core-induced azimuthal current, we would like to provide additional informations which are not easily observed by the analytical expressions for it. So, in order to full fill this lack, in the rest of this section we will develop some numerical evaluations.

In Fig. 1 we display the dependence of the core-induced azimuthal current density,  $\langle j^\phi(r) \rangle_c$ , as function of  $mr$  considering  $q = 1.5$  and  $ma = 1$ . On the left plot, we present the behavior for the current induced by the cylindrical shell of magnetic field, taking into account positive and negative value for  $\alpha$ . In order to provide a better understanding about this current, on the right plot we exhibit its behavior as function of  $mr$ , for the three different models of magnetic fields considering  $\alpha = 2.1$ . By this plot we can infer that for a given point outside the tube, the intensity of the current induced by the first model is the biggest one.

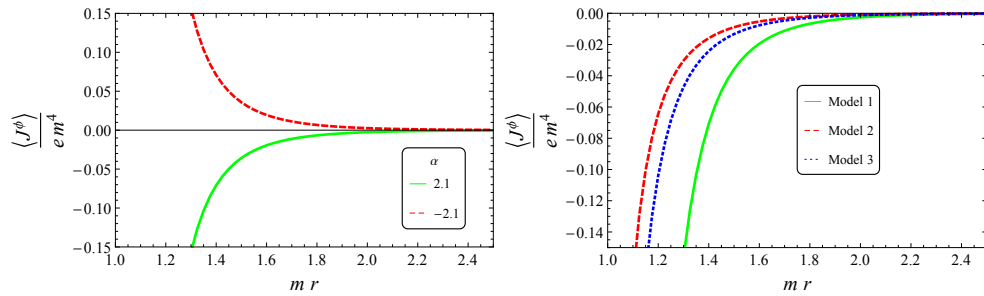


Figure 1: The core-induced azimuthal current density is plotted, in units of “ $m^4 e$ ”, as function of  $mr$  for the values  $q = 1.5$  and  $ma = 1$ . In the left plot we consider the current induced by the magnetic field configuration of the first model, and taking  $\alpha = 2.1$  and  $\alpha = -2.1$ . On the right plot we compare the intensity of the core-induced current for the three different models of magnetic fields considering  $\alpha = 2.1$ .

Another analysis that deserves to be developed is related with dependence of the core-induced azimuthal current with the parameter which codifies the presence of the cosmic string,  $q$ . So, in Fig 2, we display, for the magnetic field concentrated in a cylindrical shell, the behavior of

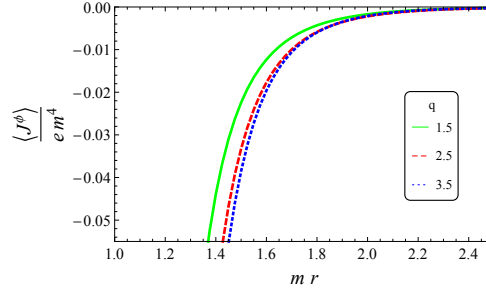


Figure 2: The core-induced azimuthal current density in units of “ $m^4 e$ ”, due to a magnetic field concentrated on a shell, as function of  $mr$  considering three different values of  $q$ . In this plot we adopted  $\alpha = 1.2$ .

$\langle j^\phi(r) \rangle_c$  as function of  $mr$  for  $q = 1.5, 2.5, 3.5$ . As we can see the intensity of the current increases with  $q$ . For this plot we consider  $\alpha = 1.2$  and  $ma = 1$ .

Finally in Fig 3 we exhibit the behavior of the core-induced current as function of  $\alpha$ , considering  $ma = 1$  and  $mr = 2$ . In the left plot, we display the current induced by the first model of magnetic field and different values of  $q$ . These values are  $q = 1.5, 2.0, 3.5$ . In the right plot we consider the currents induced by the three different models, adopting  $q = 1.5$ . For both plots, we assume that  $\alpha$  varies in the interval  $[-7.0, 7.0]$ . From both plots we can infer once more that, the intensity of the current increases with  $q$  (left plot) and the first model provide the current with biggest intensity (right plot).

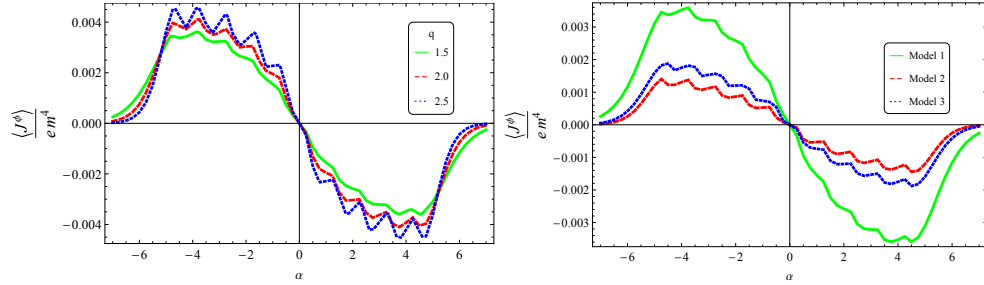


Figure 3: The core-induced azimuthal current density is plotted, in units of “ $m^4 e$ ”, as function of  $\alpha$  for  $ma = 1$  and  $mr = 2$ . In the left plot, we exhibit only the current induced by the first model considering different values of  $q$ , and in the right plot, we exhibit the current induced by the three different models of magnetic fields, considering  $q = 1.5$ .

## 4 Conclusions

In this paper we have investigated the influence of the conical topology of the spacetime and the finite core effect on the vacuum expectation value of fermionic current densities induced by magnetic fluxes. In the model considered we have adopted that the geometry of the spacetime corresponds to an idealized cosmic string everywhere, surrounded by a magnetic tube of radius  $a$ . In this tube three different configurations of magnetic fields have been taken into account: a cylindrical shell, a field decaying with  $1/r$  and finally a homogeneous magnetic field. In order to develop these analysis we had to construct the normalized fermionic wave-function for the region outside the tube, and calculated the fermionic current densities by using the mode summation

method, as shown in (3.1) and (3.2). This complete set of the fermionic wave-function was constructed by imposing continuity condition for the wave-functions in the regions inside and outside the tube, at the boundary,  $r = a$ . These functions were given by (2.35) and (2.45), respectively. As to the normalization condition, it determines the values of the interior radial functions at the boundary, see (2.43).

Although the magnetic field vanishes outside the tube, the magnetic field inside the tube induced a non-vanishing only an azimuthal current density in the exterior region. This outside current is consequence of two type of effects: the Aharonov-Bohm-like effect, and the direct interaction of the charged fermionic field with the magnetic field inside the core. This phenomenon is explicitly manifested in the structure of the induced current. The latter been decomposed in two distinct contributions: The first one depends only on the fractional part of the ratio of the total magnetic flux by the quantum one. It is given in (3.25) and is a periodic function of the total flux with the period equal to quantum flux. The second contribution named core-induced given by (3.30), in general is not a periodic function of the magnetic flux and depends on the total magnetic flux inside the core. By general analysis we could observe that the core-induced azimuthal current decays with  $e^{-2mr}/(mr)^3$  for  $mr \gg 1$  (see (3.32)). For the zero-thickness azimuthal current the corresponding decay is  $e^{-2mr \sin(\pi/q)}/(mr)^{5/2}$  for  $q > 2$ , consequently the latter dominates the total azimuthal current. For  $q \leq 2$ , both contributions are of the same order. We have also analyzed the core-induced current for two other asymptotic regions of the parameters. In these analysis we have explicitly used the solutions for the radial function inside the tube for the three different models of magnetic flux.<sup>4</sup> For massless field and at large distance from the core, the result was given by Eq. (3.45), and explicitly we see that this current decays with  $\frac{1}{r^4(a/r)^{2\beta}}$  for large distance from the tube. Comparing this result with the corresponding one for the massless limit of the zero-thickness azimuthal current wiche decays with  $1/r^4$ , we conclude that for large distance the total azimuthal current, is dominated by the zero-thickness contribution. For point near the tube core, the core-induced current diverges with  $\frac{1}{r^4(1-a/r)^3}$ , as shown by (3.53). So this contribution is dominant in this region.

Finally we have also provide, by using numerical evaluation, the behavior of the core-induced current as function of several physical quantities relevant in our analysis. In figure 1 we have two plots. In the left plot an expected result is presented. The current changes its sign when we change the sign of  $\alpha$ . In the right plot, it is exhibited the behavior of the current for the three models as function of  $mr$ . It is shown that the intensity of the current induced by the first model is the biggest one. In figure 2, we exhibit the behavior of current density for the first model as function of  $mr$  and fixed value of  $\alpha$  for different values of  $q$ . By this plot we can infer that increasing  $q$  the intensity of the current also increases. (Although this latter numerical analysis was presented only for the first model, for the other two models the current behaves in a similar way.) In figure 3, we have displayed current as function of the intensity of the magnetic flux. In the left plot we have considered only the first model fixed  $mr$  and varying  $q$ . This plot reinforces the fact that the intensity of the current increases with  $q$ ; moreover, it shows that the current is not a periodic function of the flux. The right plot exhibits the behavior of the core-induced current, for the three models, for fixed value of  $q$ . Also this plot reinforce that the first model provides the current with biggest intensity.<sup>5</sup>

**Acknowledgments:** We thank Coordenação de Aperfeiçoamento de Pessoal de Nível Superior (CAPES) and Conselho Nacional de Desenvolvimento Científico e Tecnológico (CNPq) for partial financial support.

<sup>4</sup>The radial solutions for the region inside the core, were possible by the obtainment of recurrence relations involving Whittaker function  $M_{\kappa,\lambda}(z)$  given in the Appendix A.

<sup>5</sup>In all numerical analysis it was consideres  $ma = 1$ .

## A Recurrence relations for the radial

In this appendix we shall develop explicitly the radial differential equations satisfied by functions  $R_1(r)$  and  $R_2(r)$ , considering the three configurations of magnetic fields given by the ansatz (2.15) in (2.16):

$$\left[ r^2 \lambda^2 - \left( qj + eA_\phi^{(i)} - \frac{1}{2} \right)^2 - er^2 B^{(i)}(r) \right] R_1(r) + r^2 R_1''(r) + r R_1'(r) = 0 , \quad (\text{A.1})$$

$$\left[ r^2 \lambda^2 - \left( qj + eA_\phi^{(i)} + \frac{1}{2} \right)^2 + er^2 B^{(i)}(r) \right] R_2(r) + r^2 R_2''(r) + r R_2'(r) = 0 , \quad (\text{A.2})$$

where the upper index  $i = 1, 2, 3$  characterizes which model we are working.

Now we have the general system of equation to the inside situation for each kind of magnetic field that we are working the above equation will provide different types of solution to the radial functions.

### A.1 The cylindrical shell of magnetic field

For this case we have for the vector potential

$$A_\phi^{(1)} = -q \frac{\Phi}{2\pi} \Theta(r - a) . \quad (\text{A.3})$$

For this case, in the the region  $r < a$ , both vector potential and magnetic field vanish. So the equations (A.1) and (A.2) reads,

$$\left[ r^2 \lambda^2 - \left( qj - \frac{1}{2} \right)^2 \right] R_1(r) + r^2 R_1''(r) + r R_1'(r) = 0 , \quad (\text{A.4})$$

$$\left[ r^2 \lambda^2 - \left( qj + \frac{1}{2} \right)^2 \right] R_2(r) + r^2 R_2''(r) + r R_2'(r) = 0 . \quad (\text{A.5})$$

The regular solutions at origin,  $r = 0$ , are the first kind Bessel functions. So, for the upper components of the fermionic wave-function we have

$$\psi_+ = e^{ikz} e^{iqn\phi} \begin{pmatrix} a J_{\nu_j}(\lambda r) \\ b J_{\nu_j + \tilde{\epsilon}_j}(\lambda r) e^{iq\phi} \end{pmatrix} , \quad (\text{A.6})$$

where  $\nu_j = q|j| - \frac{\tilde{\epsilon}_j}{2}$ , with  $\tilde{\epsilon}_j = 1$  for  $j > 0$  and  $\tilde{\epsilon}_j = -1$  for  $j < 0$ . The lower component is found when we substitute the above solution into (2.16), then we find

$$\psi_- = \frac{-ie^{ikz} e^{iqn\phi}}{(E + m)} \begin{pmatrix} \lambda b [J'_{\nu_j + \tilde{\epsilon}_j}(\lambda r) + \frac{\nu_j + \epsilon_j}{\lambda r} J_{\nu_j + \tilde{\epsilon}_j}(\lambda r)] + ika J_{\nu_j}(\lambda r) \\ \{\lambda a [J'_{\nu_j}(\lambda r) - \frac{\nu_j}{\lambda r} J_{\nu_j}(\lambda r)] - ikb J_{\nu_j + \tilde{\epsilon}_j}(\lambda r)\} e^{iq\phi} \end{pmatrix} . \quad (\text{A.7})$$

By using the recurrence relations involving the Bessel functions [29], we can write:

$$\psi_- = e^{ikz} e^{iqn\phi} \begin{pmatrix} c J_{\nu_j}(\lambda r) \\ d J_{\nu_j + \tilde{\epsilon}_j}(\lambda r) e^{iq\phi} \end{pmatrix} , \quad (\text{A.8})$$

where the new coefficients  $c$  and  $d$  are given below,

$$c = \frac{ka - i\epsilon_j \lambda b}{E + m} \quad (\text{A.9})$$

$$d = -\frac{kb - i\epsilon_j \lambda a}{E + m} \quad (\text{A.10})$$

## A.2 The magnetic field decays with $1/r$

For this case we have the vector potential given by

$$A_\phi^{(2)} = -q \frac{\Phi r}{2\pi a} . \quad (\text{A.11})$$

The magnetic field is  $B^{(2)} = -q \frac{\Phi}{2\pi ar}$ . So by (A.1) and (A.2) follow that,

$$\left[ r^2 \lambda^2 - \left( qj + q\alpha \frac{r}{a} - \frac{1}{2} \right)^2 - \frac{q\alpha r}{a} \right] R_1(r) + r^2 R_1''(r) + r R_1'(r) = 0 , \quad (\text{A.12})$$

$$\left[ r^2 \lambda^2 - \left( qj + q\alpha \frac{r}{a} + \frac{1}{2} \right)^2 + \frac{q\alpha r}{a} \right] R_2(r) + r^2 R_2''(r) + r R_2'(r) = 0 . \quad (\text{A.13})$$

The regular solutions at origin of above equations are the Whittaker function  $M_{\kappa, \lambda}(z)$ . So, for the upper component we have

$$\psi_+ = \frac{e^{ikz} e^{iqn\phi}}{\sqrt{r}} \begin{pmatrix} c_1 M_{\kappa, \nu_j}(\xi r) \\ c_2 M_{\kappa, \nu_j + \tilde{\epsilon}_j}(\xi r) e^{iq\phi} \end{pmatrix} , \quad (\text{A.14})$$

where the parameters  $\kappa$  and  $\xi$  are given in (3.35). The lower component is found when we substitute the above solution into (2.16). We have:

$$\psi_- = \frac{-ie^{ikz} e^{iqn\phi}}{(E+m)\sqrt{r}} \begin{pmatrix} \xi c_2 [M'_{\kappa, \nu_j + \tilde{\epsilon}_j}(\xi r) + \frac{qj + \alpha r/a}{\xi r} M_{\kappa, \nu_j + \tilde{\epsilon}_j}(\xi r)] + ikc_1 M_{\kappa, \nu_j}(\xi r) \\ \{ \xi c_1 [M'_{\kappa, \nu_j}(\xi r) - \frac{qj + \alpha r/a}{\xi r} M_{\kappa, \nu_j}(\xi r)] - ikc_2 M_{\kappa, \nu_j + \tilde{\epsilon}_j}(\xi r) \} e^{iq\phi} \end{pmatrix} . \quad (\text{A.15})$$

Unfortunately, we did not find in the literature any recurrence relation involving this kind of Whittaker functions which allows us to express the lower components in a simpler form. So, by expressing these functions in terms of Confluent Hypergeometric Functions, and by using the computer program MAPLE, we could construct the following relations:

- For  $j > 0$ , we have,

$$M'_{\kappa, \nu_j + 1}(z) + \left( \frac{\nu_j + 1/2}{z} - \frac{\kappa}{2\nu_j + 1} \right) M_{\kappa, \nu_j + 1}(z) = c_j^{(+)} M_{\kappa, \nu_j}(z) , \quad (\text{A.16})$$

$$M'_{\kappa, \nu_j}(z) - \left( \frac{\nu_j + 1/2}{z} - \frac{\kappa}{2\nu_j + 1} \right) M_{\kappa, \nu_j}(z) = c_j^{(-)} M_{\kappa, \nu_j + 1}(z) . \quad (\text{A.17})$$

- For  $j < 0$ , we have:

$$M'_{\kappa, \nu_j - 1}(z) - \left( \frac{\nu_j - 1/2}{z} - \frac{\kappa}{2\nu_j - 1} \right) M_{\kappa, \nu_j - 1}(z) = c_j^{(+)} M_{\kappa, \nu_j}(z) , \quad (\text{A.18})$$

$$M'_{\kappa, \nu_j}(z) + \left( \frac{\nu_j - 1/2}{z} - \frac{\kappa}{2\nu_j - 1} \right) M_{\kappa, \nu_j}(z) = c_j^{(-)} M_{\kappa, \nu_j - 1}(z) . \quad (\text{A.19})$$

In the above expressions the coefficients  $c_j^{(\pm)}$  are given below:

$$c_j^{(+)} = \begin{cases} 2(\nu_j + 1) , & j > 0 . \\ \frac{1}{8\nu_j} \left[ 1 - \left( \frac{2\kappa}{2\nu_j + 1} \right)^2 \right] , & j < 0 . \end{cases} \quad (\text{A.20})$$

$$c_j^{(-)} = \begin{cases} -\frac{1}{8(\nu_j + 1)} \left[ 1 - \left( \frac{2\kappa}{2\nu_j + 1} \right)^2 \right] , & j > 0 . \\ 2\nu_j , & j < 0 . \end{cases} \quad (\text{A.21})$$

Finally we can write the Dirac wave-function with positive-energy into the form below

$$\psi^{(+)}(x) = \frac{e^{-ipx} e^{iqn\phi}}{\sqrt{r}} \begin{pmatrix} c_1 M_{\kappa, \nu_j}(\xi r) \\ c_2 M_{\kappa, \nu_j + \tilde{\epsilon}_j}(\xi r) e^{iq\phi} \\ \tilde{c}_1 M_{\kappa, \nu_j}(\xi r) \\ \tilde{c}_2 M_{\kappa, \nu_j + \tilde{\epsilon}_j}(\xi r) e^{iq\phi} \end{pmatrix}, \quad (\text{A.22})$$

where

$$\tilde{c}_1 = \frac{kc_1 - ic_2 c_j^{(+)}}{E + m} \quad \tilde{c}_2 = -\frac{kc_2 + ic_1 c_j^{(-)}}{E + m}. \quad (\text{A.23})$$

### A.3 The homogeneous magnetic field

Our last analysis is for uniform magnetic field. In this case the azimuthal component of the vector potential is,

$$A_\phi^{(3)}(r) = -\frac{q\Phi}{2\pi} \left(\frac{r}{a}\right)^2. \quad (\text{A.24})$$

The magnetic fields is  $B^{(3)} = -\frac{2q\Phi}{2\pi a^2}$ . Following the same proceeding as before, the solutions will be also given in terms of the regular at origin Whittaker functions. For the upper component we have

$$\psi_+ = \frac{e^{ikz} e^{iqn\phi}}{r} \begin{pmatrix} c_1 M_{\kappa - \frac{1}{4}, \frac{\nu_j}{2}}(\tau r^2) \\ c_2 M_{\kappa + \frac{1}{4}, \frac{\nu_j + \tilde{\epsilon}_j}{2}}(\tau r^2) e^{iq\phi} \end{pmatrix}, \quad (\text{A.25})$$

where  $\tau$  and  $\kappa$  are given by

$$\tau = q\alpha/a^2, \quad \kappa = \frac{\lambda^2}{4\tau} - \frac{qj}{2}. \quad (\text{A.26})$$

Substituting (A.25) into (2.16) we have the lower component given by

$$\psi_- = \frac{-ie^{ikz} e^{iqn\phi}}{(E + m)r} \begin{pmatrix} c_2 \left( \frac{qj - \frac{1}{2}}{r} + \tau r + \partial_r \right) M_{\kappa^+, \frac{\nu_j}{2}}(\tau r) + ikc_1 M_{\kappa^-, \frac{\nu_j}{2}}(\tau r) \\ \{c_1 \left( \partial_r - \frac{qj - \frac{1}{2} + \tau r^2}{r} \right) M_{\kappa^-, \frac{\nu_j}{2}}(\tau r) - ikc_2 M_{\kappa^+, \frac{\nu_j}{2}}(\tau r)\} e^{iq\phi} \end{pmatrix}. \quad (\text{A.27})$$

Also we have not found in literature the recurrence relations involving the Whittaker functions necessary for us to express the (A.27) in a simpler form. So, by using the same procedure explained in the last analysis we were able to find the following recurrence relations:

- For  $j > 0$ :

$$\left( \frac{\nu_j}{2\tau} + \frac{1}{2} + \frac{d}{dz} \right) M_{\kappa + \frac{1}{4}, \frac{\nu_j + 1}{2}}(z) = \frac{c_j^{(+)}}{2\sqrt{z}} M_{\kappa - \frac{1}{4}, \frac{\nu_j}{2}}(z), \quad (\text{A.28})$$

$$\left( -\frac{\nu_j}{2\tau} + \frac{1}{2} + \frac{d}{dz} \right) M_{\kappa - \frac{1}{4}, \frac{\nu_j}{2}}(z) = \frac{c_j^{(-)}}{2\sqrt{z}} M_{\kappa + \frac{1}{4}, \frac{\nu_j + 1}{2}}(z). \quad (\text{A.29})$$

- For  $j < 0$

$$\left( -\frac{\nu_j + 1}{2\tau} + \frac{1}{2} + \frac{d}{dz} \right) M_{\kappa + \frac{1}{4}, \frac{\nu_j - 1}{2}}(z) = \frac{c_j^{(+)}}{2\sqrt{z}} M_{\kappa - \frac{1}{4}, \frac{\nu_j}{2}}(z), \quad (\text{A.30})$$

$$\left( \frac{\nu_j + 1}{2\tau} + \frac{1}{2} + \frac{d}{dz} \right) M_{\kappa - \frac{1}{4}, \frac{\nu_j}{2}}(z) = \frac{c_j^{(-)}}{2\sqrt{z}} M_{\kappa + \frac{1}{4}, \frac{\nu_j - 1}{2}}(z). \quad (\text{A.31})$$

In the above expressions,  $c_j^{(\pm)}$  are given by,

$$c_j^{(+)} = \begin{cases} 2(\nu_j + 1), & j > 0 \\ \left(1 - \frac{4\kappa+1}{2(\nu_j+1)}\right), & j < 0 \end{cases} \quad (\text{A.32})$$

$$c_j^{(-)} = \begin{cases} -\left(1 + \frac{4\kappa-1}{2\nu_j}\right), & j > 0 \\ 2\nu_j, & j < 0 \end{cases} \quad (\text{A.33})$$

Finally for the third model we have the positive-energy wave-function written below

$$\psi^{(+)}(x) = \frac{e^{-ipx} e^{iqn\phi}}{r} \begin{pmatrix} c_1 M_{\kappa^-, \frac{\nu_j}{2}}(\tau r^2) \\ c_2 M_{\kappa^+, \frac{\tilde{\nu}_j}{2}}(\tau r^2) e^{iq\phi} \\ \tilde{c}_1 M_{\kappa^-, \frac{\nu_j}{2}}(\tau r^2) \\ \tilde{c}_2 M_{\kappa^+, \frac{\tilde{\nu}_j}{2}}(\tau r^2) e^{iq\phi} \end{pmatrix}, \quad (\text{A.34})$$

where  $\tilde{c}_{1,2}$  are also given by (A.23).

#### A.4 Analysis of the coefficient $\mathcal{V}_j^{(i)}$

To prove (3.8) we shall use its explicit form given bellow:

$$\mathcal{V}_j^{(i)}(\pm i\lambda, a) = \frac{R_2^{(i)}(r)}{R_1^{(i)}(r)}. \quad (\text{A.35})$$

For the first model we have

$$\mathcal{V}_j^{(1)}(\pm i\lambda, a) = \tilde{\epsilon}_j \frac{J_{\tilde{\nu}_j}(i\lambda a)}{J_{\nu_j}(i\lambda a)}. \quad (\text{A.36})$$

Using the well know relation involving the Bessel function with imaginary argument and the modified Bessel function [29], the above equation becomes

$$\mathcal{V}_j^{(1)}(\pm i\lambda, a) = \tilde{\epsilon}_j(\pm i)^{\tilde{\epsilon}_j} \frac{I_{\tilde{\nu}_j}(\lambda a)}{I_{\nu_j}(\lambda a)}. \quad (\text{A.37})$$

We notice that, for positive or negatives values of  $j$ ,  $\tilde{\epsilon}_j = \pm 1$ , consequently  $\tilde{\epsilon}_j(\pm i)^{\tilde{\epsilon}_j} = \pm i$ . In this way we have:

$$\mathcal{V}_j^{(1)}(\pm i\lambda, a) = \pm i \text{Im}[\mathcal{V}_j^{(1)}(i\lambda, a)]. \quad (\text{A.38})$$

For the others two models, the procedure to show (3.8) is similar. Specifically for the second model, we can use (3.34)-(3.36). So, we have

$$\mathcal{V}_j^{(2)}(\pm i\lambda, a) = c_j^{(2)} \frac{M_{\kappa, \tilde{\nu}_j}(\xi a)}{M_{\kappa, \nu_j}(\xi a)}. \quad (\text{A.39})$$

Taking  $\lambda \rightarrow \pm i\lambda$  we obtain:

- For positive values of  $j$

$$c_j^{(2)} = \frac{(\pm i\lambda)}{\xi} \frac{1}{2q|j|+1} = \pm i \text{Im}[c_j^{(2)}] \quad (\text{A.40})$$

- For negative values of  $j$

$$c_j^{(2)} = -\frac{\xi}{\pm i\lambda}(2q|j| + 1) = \pm i\text{Im}[c_j^{(2)}] . \quad (\text{A.41})$$

Consequently, for the second model, we get

$$\mathcal{V}_j^{(2)}(\pm i\lambda, a) = c_j^{(2)} \frac{M_{\kappa, \tilde{\nu}_j}(\xi a)}{M_{\kappa, \nu_j}(\xi a)} = \pm i\text{Im}[\mathcal{V}_j^{(2)}(i\lambda, a)] . \quad (\text{A.42})$$

Finally for the third model, we can easily show that the relation (3.8) holds.

## References

- [1] A. A. Abrikosov, Zh. Eksp. Teor. Fiz. **32**, 1442 (1957).
- [2] N.B. Nielsen, P. Olesen, Nucl. Phys. B **61**, 45 (1973).
- [3] D. Garfinkle, Phys. Rev. D **31** 1323 (1985).
- [4] P. Laguna-Castillo and R. A. Matzner, Phys. Rev. D **35** 2933 (1987).
- [5] B. Linet, Phys. Lett. A **124**, 240 (1987).
- [6] A. Vilenkin, E.P.S. Shellard, *Cosmic String and Other Topological Defects*, Cambridge University Press, Cambridge (1994).
- [7] V. Berezhinski, B. Hnatyk, A. Vilenkin, Phys. Rev. D **64**, 043004 (2001)
- [8] T. Damour, A. Vilenkin, Phys. Rev. Lett. **85**, 3761 (2000)
- [9] P. Bahttacharjee, G. Sigl, Phys. Rep. **327**, 109 (2000).
- [10] E.R. Bezerra de Mello, V.B. Bezerra, A.A. Saharian, and A.S. Tarloyan, Phys. Rev. D **74**, 025017 (2006).
- [11] J.S. Dowker, Phys. Rev. D **36**, 3742 (1987).
- [12] M.E.X. Guimarães and B. Linet, Commun. Math. Phys. **165**, 297 (1994); M.E.X. Guimarães, Class. Quantum Grav. **12**, 1705 (1995); B. Linet, Class. Quantum Grav. **13**, 97 (1996).
- [13] J. Spinelly and E. R. Bezerra de Mello, JHEP **09**, 005 (2008).
- [14] Yu.A. Sitenko and N.D. Vlasii, Class. Quantum Grav. **29**, 095002 (2012).
- [15] L. Sriramkumar, Class. Quantum Grav. **18**, 1015 (2001).
- [16] Yu.A. Sitenko and N.D. Vlasii, Class. Quantum Grav. **26**, 195009 (2009).
- [17] E.R. Bezerra de Mello, Class. Quantum Grav. **27**, 095017 (2010).
- [18] E.R. Bezerra de Mello and A.A. Saharian, Eur. Phys. J. C **73**, 2532 (2013).
- [19] E. A. F. Bragança, H. F. Santana Mota and E. R. Bezerra de Mello, Int. J. Mod. Phys. D **24**, 1550055 (2015)
- [20] J. Spinelly and E.R. Bezerra de Mello, Class. Quantum Grav. **20** 874, (2003).
- [21] J. Spinelly and E.R. Bezerra de Mello, Int. J. Mod. Phys. D **13**, 607 (2004); J. Spinelly and E.R. Bezerra de Mello, Nucl Phys. B (Proc. Suppl.) **127**, 77 (2004).
- [22] B. Allen, B.S. Kay, A.C. Ottewill, Phys. Rev. D **53**, 6829 (1996)
- [23] E. R. Bezerra de Mello, V. B. Bezerra, A. A. Saharian and H. H. Harutyunyan, Phs. Rev. D **91**, 064034 (2015).
- [24] M. Bordag and S. Voropaev, J. Phys. A: Math. Gen. **26**, 7637 (1993).
- [25] M. Bordag and S. Voropaev, Phys. Lett. B **333**, 238 (1994).

- [26] M. Bordag and N. Khusnutdinov, *Classical Quantum Gravity* **13**, L41 (1996).
- [27] J. D. Bjorken and S. D. Drell, *Relativistic Quantum Mechanics* (McGraw-Hill, Inc. 1964).
- [28] E.R. Bezerra de Mello and A.A. Saharian, *Eur. Phys. J. C.* **73**, 2532 (2013)
- [29] M. Abramowitz and I. A. Stegun, *Handbook of Mathematical Functions* (National Bureau of Standards, Washington DC, 1964).
- [30] I. S. Gradshteyn and I. M. Ryzhik, *Table of Integrals, Series and Products* (Academic Press, New York, 1980).
- [31] E.R. Bezerra de Mello, V.B. Bezerra, A.A. Saharian, and V.M. Bardeghyan, *Phys. Rev. D* **82**, 085033 (2010)